Residue Effect of Parallel Interference Canceller in Belief Propagation Decoding in Massive MIMO Systems

Kazuyuki Sakoda[1,2], Hiroki Hata[2], and Shigefumi Hata[2]
[1] Department of Electrical and Computer Engineering, Miyakonojo College, Miyazaki, Japan
[2] Graduate School of Science and Engineering, Kagoshima University, Kagoshima, Japan
Email: sakoda@cc.miyakonojo-nct.ac.jp; {hata; sighata}@sci.kagoshima-u.ac.jp

***Abstract*—Belief-Propagation (BP) iterative decoding is considered in massive Multiple-Input Multiple-Output (MIMO) wireless communication systems. A problem with this BP decoding method that has yet to be solved is the evaluation of the residues in the Parallel Interference Canceller (PIC), which cannot be calculated directly. Furthermore, although there are various methods through which the residue effect may be accounted for, no comparative studies have thus far been reported. Hence, in this study, we consider the residue component as a random variable and construct BP decoders in which the residue effect is included into the likelihood of the PIC in different ways. We numerically compare the decoding performance among them. The results suggest that the decoder has high performance when it contains the residue effect in the variance of the likelihood.**

***Index Terms*—Belief propagation, iterative decoding, massive MIMO**

I. Introduction

Multiple-Input Multiple-Output (MIMO) wireless communication systems employ multiple transmitting and receiving antennas to achieve high-capacity data transmission [1]. To further enhance capacity, researchers have recently begun investigating extensively MIMO systems using 10–100 antennas (massive MIMO) [2]–[7]. However, such massive systems experience an inherent increase in the computation time required for decoding. When employing Maximum Likelihood Decoding (MLD), a standard decoding technique in wireless communication, the computation time is generally proportional to the modulation level to the power of the number of antennas, which is not practical to be used in massive MIMOs [5]–[7]. Therefore, alternative decoding methods are being explored to reduce computational costs. QR-decomposition and M-algorithm have been applied to MLD to reduce computation time [8], [9]; further, iterative estimation schemes have been considered instead of MLD for predicting true data [10]–[21]. In particular, the computation time of Belief Propagation (BP) iterative estimation is proportional to the number of antennas raised to the second power, which is applicable even for massive MIMO systems. The BP method is also advantageous because if the number of antennas is sufficiently large, it can accurately estimate without error-correcting code, which makes it a competitive option for massive MIMO systems [14]–[19].

A problem with the current BP decoding method is the evaluation of residues in the Parallel Interference Canceller (PIC) [16], [17]. As we will further detail in the methods section, the BP decoder estimates true data based on the PIC. By constructing single-input multiple-output channels for each receiving antenna, the likelihood of the PIC is calculated to evaluate the plausibility of the estimate. By updating the PIC iteratively, the most plausible data set is found, which achieves the current state of the transmitting and receiving antennas. The interference is cancelled completely when the decoder finds the true data, however, residue remains in the searching process, which cannot be calculated directly. Previous studies have therefore treated this component as a random variable and included its effect into the likelihood of the PIC in several ways [16]–[21].

This paper presents the results of a comparative study on residue components in the BP decoder. Although we have choices for how to consider the residue effect in the likelihood function, no comparative analysis has thus far reported. Hence, we consider in this study BP decoders for which the residue effect is included into the mean, or variance, or both, of the likelihood. We then numerically evaluate the accuracy of each decoder and compare the decoding performance.

II. Method

We consider a massive MIMO system composed of N_t-transmitting and N_r-receiving antennas. Transmitted bit data are modulated by the Binary Phase Shift Keying (BPSK) and are sent to the receiving antenna. The receiver then estimates the true bits from the received signals by using the BP decoder (Fig. 1).

Manuscript received May 16, 2019; revised June 19, 2019; accepted July 12, 2019.

Corresponding author: K. Sakoda (sakoda@cc.miyakonojo-nct.ac.jp).

doi: 10.18178/ijeetc.9.1.13-17

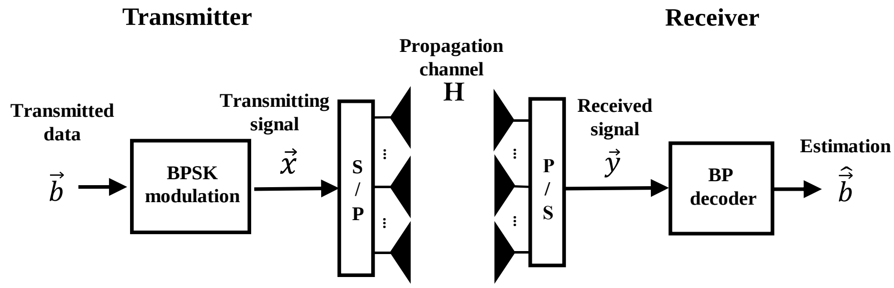

Fig. 1. BP decoding applied to massive MIMO.

A. Massive MIMO

A set of bit data is represented as a vector

$$\vec{b} = \left(b_1, b_2, \ldots, b_{N_t}\right) \tag{1}$$

where $b_i \in \{0,1\}$ for i = 1, 2, ⋯, N_t. Each single bit b_i is modulated by the BPSK to transmitted signal x_i as follows:

$$\vec{x} = \left(x_1, x_2, \cdots, x_{N_t}\right) \tag{2}$$

where

$$x_i = \begin{cases} 1 \ (b_i = 1) \\ -1 \ (b_i = 0) \end{cases} \text{ for } i = 1, 2, \cdots, N_t$$

Each element of $\vec{x}$ is assigned to a transmitting antenna and sent to the receiving antennas via a multi-path propagating channel described by **H**. The received signal $\vec{y}$ is therefore given by

$$\vec{y} = \mathbf{H}\vec{x} + \vec{n} \tag{3}$$

where $\vec{n}$ represents the effect of noise.

B. BP Decoder

Fig. 2 (a) exhibits the Tanner graph of our massive MIMO system. The receiver decodes the received signal $\vec{y}$ by estimating the true bit set $\vec{b}$. We assume that the channel matrix **H** is perfectly known at the receiver. The estimate $\vec{b}$ is thus given as a function of $\vec{y}$ and **H**, i.e., $\vec{b} = \vec{b}$ ($\vec{y}$, **H**).

The BP decoder estimates true bits based on the PIC. By constructing single-input multiple-output channels for each observation node, the likelihood of the PIC is calculated to evaluate the plausibility of the estimate. By updating the PIC iteratively, a bit set is found by updating the PIC iteratively, which is the most plausible for achieving the current relationship between the symbol and observation nodes. We show in this section a standard framework of the BP method in massive MIMOs [15].

1) Process in observation nodes: The likelihood of the PIC given a bit set is calculated at each observation node (Fig. 2 (b)). The PIC $\tilde{y}_{jk}^{(l)}$ passing between the kth symbol and the jth observation node is defined by using the replica signal $\tilde{x}_{ji}^{(l)}$ as

$$\tilde{y}_{jk}^{(l)} = y_j - \sum_{i=1, i\neq k}^{N_t} h_{ji}\tilde{x}_{ji}^{(l)} \tag{4}$$

$$\tilde{x}_{ji}^{(l)} = \tanh\left(\frac{\beta_{ji}^{(l)}}{2}\right) \tag{5}$$

where the index l=1, 2, ⋯ represents the number of iterations in the BP estimation. The parameter $\beta_{ji}^{(l)}$, obtained in the previous BP iteration (See (13)), describes the reliability of the replica signal in such a way that the value replica $\tilde{x}_{ji}^{(l)}$ approaches the true data value x_j=1 or −1 when the magnitude of $\beta_{ji}^{(l)}$ increases.

Equation (4) is also written as follows:

$$\tilde{y}_{jk}^{(l)} = h_{jk}x_k + n_j + R_{jk}^{(l)} \tag{6}$$

$$R_{jk}^{(l)} = \sum_{i=1, i\neq k}^{N_t} h_{ji}\left(x_i - \tilde{x}_{ji}^{(l)}\right). \tag{7}$$

The residue component $R_{jk}^{(l)}$ cannot be calculated because it depends on the true bit value b_k which is unknown to the receiver. Previous studies therefore treated this component as a random variable and included its effect into the likelihood function of the PIC:

$$\Pr\left(\tilde{y}_{jk}^{(l)} | x_k\left(b_k\right)\right) = N\left(\tilde{y}_{jk}^{(l)} | h_{jk}x_k + \mu_{jk}^{(l)}, \sigma_{jk}^{(l)2} + \sigma_n^2\right) \tag{8}$$

where $N\left(*|\mu, \sigma^2\right)$ is the normal distribution with the mean μ and variance σ^2, while

$$\mu_{jk}^{(l)} = \sum_{i=1, i\neq k}^{N_t} h_{ji}\left(x_i - \tilde{x}_{ji}^{(l)}\right) \tag{9}$$

$$\sigma_{jk}^{(l)2} = \sum_{i=1, i\neq k}^{N_t} \left|h_{ji}\right|^2 \left(x_i - \tilde{x}_{ji}^{(l)}\right)^2 \tag{10}$$

represents the residue effect. The variance of this normal likelihood also contains the effect of noise σ_n^2. Note that the residue effects (9) and (10) still depend on the true bit. In Section II-C, we propose a method of evaluating them.

The log likelihood ratio (LLR)

$$\alpha_{jk}^{(l)} = \log\frac{\Pr\left(\tilde{y}_{jk}^{(l)} | x_k\left(b_k = 1\right)\right)}{\Pr\left(\tilde{y}_{jk}^{(l)} | x_k\left(b_k = 0\right)\right)} \tag{11}$$

evaluates the plausibility of the estimate by assessing the relationship of the symbol and observation nodes.

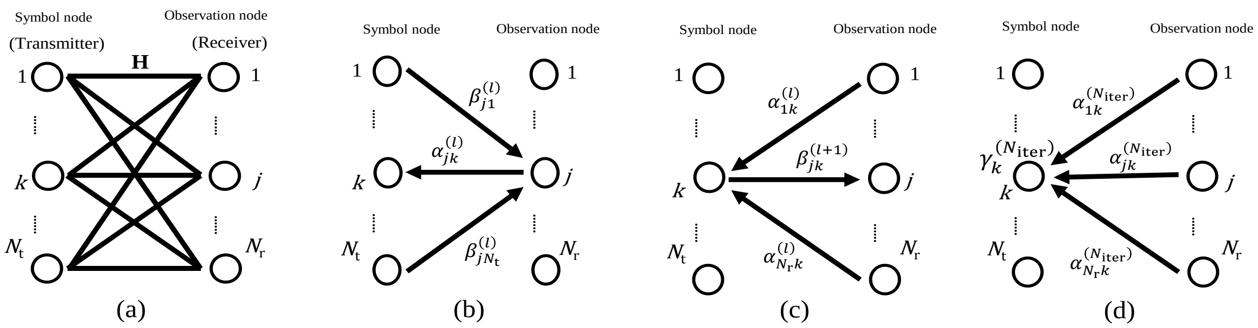

Fig. 2. MIMO system: (a) Tanner graph of massive MIMO system, (b) process in observation node, LLR $\alpha_{jk}^{(l)}$ of the PIC passing between the kth symbol and jth observation nodes is calculated, (c) process in symbol node, reliability parameter $\beta_{ji}^{(l+1)}$ of replica signal used in the PIC is calculated from the LLR, and (d) estimation of true bit b_k based on the posteriori LLR $\gamma_k^{(N_{\text{iter}})}$.

2) Process in symbol nodes: Each symbol node calculates the plausibility parameter $\beta_{jk}^{(l+1)}$ to be used in the next BP iteration (Fig. 2 (c)) with the following expression:

$$\gamma_k^{(l)} = \sum_{j=1}^{N_\text{r}} \alpha_{jk}^{(l)} \tag{12}$$

$$\beta_{jk}^{(l+1)} = \gamma_k^{(l)} - \alpha_{jk}^{(l)} \tag{13}$$

3) BP iteration: In the first iteration, the reliability parameter $\beta_{jk}^{(0)}$ and the replica $\tilde{x}_{jk}^{(0)}$ are set to zero for all j and k. The LLR $\alpha_{jk}^{(0)}$ based on the PIC is obtained by (4)–(11). The reliability parameter $\beta_{jk}^{(1)}$ is then calculated according to (12) and (13). By updating $\alpha_{jk}^{(l)}$ and $\beta_{jk}^{(1)}$ alternately, the reliability of each replica $\tilde{x}_{jk}^{(l)}$ gradually improves. After the fixed number of iterations N_{iter}, the estimate of the true bit b_k is determined from the posteriori LLR $\gamma_k^{(N_{\text{iter}})}$ as

$$\hat{b}_k = \begin{cases} 1, & \gamma_k^{(N_{\text{iter}})} \geq 0 \\ 0, & \gamma_k^{(N_{\text{iter}})} < 0. \end{cases} \tag{14}$$

C. Pseudo Residue Effect

Although the effect of residue $R_{jk}^{(l)}$ is included in the likelihood of the PIC in (8), the effects $\mu_{jk}^{(l)}$ and $\sigma_{jk}^{(l)2}$ still depend on the true bit and cannot be calculated directly (See (9) and (10)). Previous studies have considered MIMO systems where the receiver knows the true bit and calculates the residue effect [17]. The optimal performance of the BP decoder has thus been evaluated.

In this study, we instead propose an alternative method for handling the residue effect. Note that the residue $R_{jk}^{(l)}$ vanishes when the replicas $\tilde{x}_{ji}^{(l)}$ is replaced by the true signal x_i for all i. Effects $\mu_{jk}^{(l)}$ and $\sigma_{jk}^{(l)2}$ are thus required to approach 0 as the replicas converge to x_i. We relax this requirement and define the pseudo residue effect with the following expressions:

$$\tilde{\mu}_{jk}^{(l)} = \sum_{i=1, i\neq k}^{N_\text{t}} h_{ji} \left(\tilde{x}_{ji}^{(l-1)} - \tilde{x}_{ji}^{(l)} \right) \tag{15}$$

$$\tilde{\sigma}_{jk}^{(l)2} = \sum_{i=1, i\neq k}^{N_\text{t}} \left| h_{ji} \right|^2 \left(\tilde{x}_{ji}^{(l-1)} - \tilde{x}_{ji}^{(l)} \right)^2 \tag{16}$$

both of which approach 0 as the replicas converge to a certain value (not necessarily to x_i). In the first iteration (l=0), we assume that each $\tilde{x}_{ji}^{(-1)}$ is assigned 1 or −1 independently with an equal probability and thus get

$$\tilde{\mu}_{jk}^{(0)} = 0, \quad \tilde{\sigma}_{jk}^{(0)2} = \sum_{i=1, i\neq k}^{N_\text{t}} \left| h_{ji} \right|^2 \tag{17}$$

The pseudo residue effects do not depend on the true bits. The receivers can thus use the BP decoder even if the true bits are unknown.

Previous BP decoders include the residue effect in either the mean or variance of the likelihood [16]–[21]. We therefore consider three types of the BP decoders that account for the residue effects in the mean (model-(a)), variance (model-(b)), or both (model-(c)). Different likelihood functions are used instead of (8) in each model, which are given as follows:

$$\Pr\left(\tilde{y}_{jk}^{(l)} | x_k(b_k) \right) = N\left(\tilde{y}_{jk}^{(l)} | h_{jk} x_k + \mu_{jk}^{(l)}, \sigma_n^2 \right) \tag{18}$$

$$\Pr\left(\tilde{y}_{jk}^{(l)} | x_k(b_k) \right) = N\left(\tilde{y}_{jk}^{(l)} | h_{jk} x_k, \sigma_{jk}^{(l)2} + \sigma_n^2 \right) \tag{19}$$

$$\Pr\left(\tilde{y}_{jk}^{(l)} | x_k(b_k) \right) = N\left(\tilde{y}_{jk}^{(l)} | h_{jk} x_k + \mu_{jk}^{(l)}, \sigma_{jk}^{(l)2} + \sigma_n^2 \right) \tag{20}$$

TABLE I. COMPUTATION TIME FOR DECODING. EACH VALUE IS CALCULATED BY AVERAGING 100 TRIALS AND THEN NORMALIZED BY THE VALUE FOR THE MODEL-(A) OF N_{ITER}=1. THE NUMBER OF RECEIVING ANTENNAS IS SET TO N_T=N_R=12, WHILE THE NUMBER OF ITERATIONS IS SET TO N_{ITER}. NOISE VARIANCE FOR $\vec{n}$ IS SET TO σ_n^2 =10^{-2} (SNR=20 [DB]).

model \ N_{iter}	1	5	10	20	30	40
model-(a)	1	5.5	14.2	31.6	50.0	68.6
model-(b)	1.3	6.9	15.3	30.2	52.5	70.1
model-(c)	1.5	7.6	19.2	40.6	64.9	84.4

III. RESULTS

For comparing the performance of decoders (a)–(c) in massive MIMOs, we numerically calculate the bit error ratios (BERs) and computation times. In the numerical simulation, each bit b_i is assigned 0 or 1 independently with an equal probability. We assume the multi-path propagation is given by an i.i.d. Rayleigh fading channel, so that each element of matrix $\mathbf{H}$ is a complex number, the real and imaginary parts of which are drawn independently from a Gaussian distribution with a mean of 0 and a variance of 1. The noise vector $\vec{n}$ contains Gaussian white noise with a mean of 0 and a variance of σ_n^2. In each trial, random variables $\vec{b}$, $\mathbf{H}$ and $\vec{n}$ are generated and applied to all models. The numerical simulations are run on MATLAB® software.

A. Computation Time

The computation times are compared in Table I among three models. Model-(c) performs slightly slowly because it requires time to calculate both the mean and variance of the residue effect, however, no significant difference is observed among the three models. This suggests that the data rate is mainly determined by the decoding accuracy.

B. Decoding Accuracy

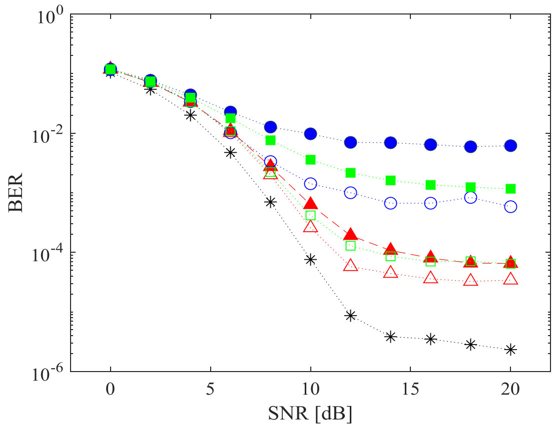

Fig. 3. The BER in massive MIMOs for model-(a) (circles), model-(b) (triangles), and model-(c) (squares). The filled symbols and open symbols respectively plot the results of N_{iter}=5 and 20. The BERs for model-(d) of N_{iter} =20 is plotted by asterisks. The numbers of antennas are set to N_t=N_r=12. Noise variance for $\vec{n}$ is given by σ_n^2 =$10^{-\text{SNR}/10}$. Each point represents mean BER averaged over 100000 trials. In all methods, each bit is modulated by the BPSK.

Fig. 3 compares the BERs at different signal-to-noise ratio (SNR) among models (a)–(c). The BERs for the BP decoder using the true residue effect, for which likelihood is given by (8)–(10) are also plotted as the performance of the optimal BP estimation (model-(d)). As can be observed in the figure, the BERs decrease as N_{iter} increases for all models. The BERs also decrease as the SNR increases. This means that all models effectively decode the received signals. In particular, model-(b) successfully exceeds the standard criteria for establishing wireless communication (BERs of ≤10^{-3}) when the SNR is larger than 10.

For models (a)–(c), the improvement of the BERs tends to plateau even if the SNR increases more than 20. This tendency may be caused by erroneous evaluation of the pseudo residue effect. In particular, for models (b) and (c), the effect is included in the variance of the likelihood (See (19) and (20)). A large value of the SNR (small value of σ_n) thus makes the residue effect relatively strong. As a result, erroneous evaluation of the residue effect more likely leads to errors in decoding.

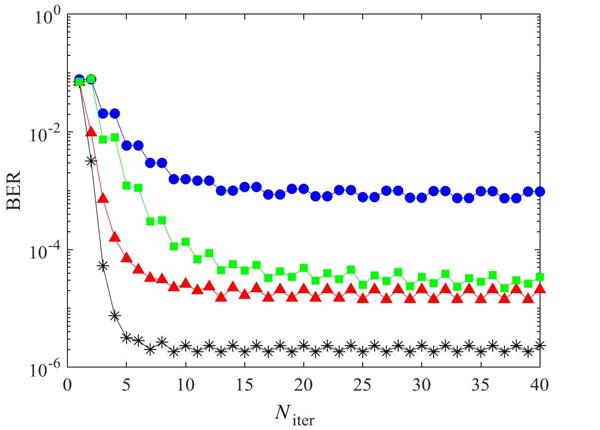

Fig. 4. The BERs in Massive MIMO for the model-(a) (circles), model-(b) (triangles), model-(c) (squares) and model-(d) (asterisks). The numbers of antennas is set to N_t=N_r=12. Noise variance for $\vec{n}$ is given by σ_n^2 =10^{-2} (SNR=20[dB]). Each point represents mean BER averaged over 100000 trials. In all methods, each bit is modulated by the BPSK.

Fig. 4 demonstrates the dependence of the BERs on the iteration number N_{iter}. As can be seen from the figure, the BERs for all models decrease gradually as N_{iter} increases. The BERs for models (b) and (c) fall quickly and converge at N_{iter}~15. On the other hand, the BERs for model-(a) decrease more slowly compared to other models. The results suggest that the BP decoder may have a higher search speed when it considers the residue effect in the variance of the likelihood.

IV. DISCUSSION AND CONCLUSIONS

In this paper, we conducted a comparative study about the residue components of the PIC in the BP decoder to be used in massive MIMO systems. The original effect cannot be calculated because it depends on the true bit. We therefore proposed a pseudo residue effect constructed from the replica signals to instead use in the BP estimation. We considered three types of BP decoders each of which respectively include the residue effect in the mean, variance, or both. We numerically evaluated the computation time and accuracy of each decoder and then compared their decoding performance. We found that the BP decoder is accurate and has a high search speed when it includes the residue effect in the variance of the likelihood.

Although model-(b) exceeds the criteria for wireless communication in terms of decoding accuracy, its BERs are still higher than those of model-(d), which uses the true signal. This means that model-(b) can still be improved. Future research may further explore how to effectively construct pseudo residues. Although we instead used the replica signal in this study, other substitutes can also be considered.

Employing higher moments of the residues in the BP decoder could also potentially expand current research. Although the mean and variance have so far been used in the BP decoder, moments of higher order may also be considered. Our results suggest the decoder performs accurately when it uses *only* the variance, i.e., the second order of the residues. Studying moments of higher order could thus be informative about the residues. We believe that the accuracy of the BP decoder can be further improved if the above points are addressed.

ACKNOWLEDGMENT

Financial support through KAKENHI (17H03279 and 19K20357) in Japan are gratefully acknowledged.

REFERENCES

[1] J. G. Proakis, *Digital Communications*, 4th ed. McGraw-Hill Education, 2001.

[2] T. L. Marzetta, "Noncooperative cellular wireless with unlimited numbers of base station antennas," *IEEE Trans. Wireless Commun.*, vol. 9, no. 11, pp. 3590–3600, 2010.

[3] F. Rusek, D. Persson, B. K. Lau, *et al*., "Scaling up MIMO: Opportunities and challenges with very large arrays," *IEEE Signal Process. Mag.*, vol. 30, no. 1, pp. 40–60, 2013.

[4] E. Telatar, "Capacity of multi-antenna Gaussian channels," *European Trans. on Telecommunications*, vol. 10, no. 6, pp. 585–595, 1999.

[5] L. Lu, G. Y. Li, A. L. Swindlehurst, *et al*., "An overview of massive MIMO: Benefits and challenges," *IEEE J. Sel. Topics Signal Process.*, vol. 8, no. 5, pp. 742–758, 2014.

[6] S. Yang and L. Hanzo, "Fifty years of MIMO detection: The road to large-scale MIMOs," *IEEE Commun. Surveys Tuts.*, vol. 17, no. 4, pp. 1941–1988, 2015.

[7] D. Araújo, T. Maksymyuk, A. L. F. Almeida, *et al*., "Massive MIMO: Survey and future research topics," *IET Commun*, vol. 10, no. 15, pp. 1938–1946, 2016.

[8] T. H. Im, J. Kim, and Y. S. Cho, "A low complexity QRM-MLD for MIMO systems," in *Proc. IEEE Vehicular Technology Conf. (VTC)*, Apr. 2007, pp. 2243–2247.

[9] H. Kawai, K. Higuchi, N. Maeda, *et al*., "Likelihood function for QRM-MLD suitable for soft-decision turbo decoding and its performance for OFCDM MIMO multiplexing in multipath fading channel," *IEICE Trans. Commun.*, vol. E88-B, no. 1, pp. 47–57, 2005.

[10] M. Wu, C. Dick, J. R. Cavallaro, *et al*., "Iterative detection and decoding in 3GPP LTE-based massive MIMO systems," presented at European Signal Processing Conf. (EUSIPCO), Sept. 2014.

[11] S. Ahmed and S. Kim, "Efficient soft bit estimation for joint iterative multiple input multiple output detection," *IET Commun.*, vol. 9, no. 17, pp. 2107–2113, 2015.

[12] S. Yoon, "Iterative detection and decoding of MIMO signals usingl low-complexity soft-in/soft-out detector," *IEICE Trans. Commun.*, vol. E98-B, no. 5, pp. 890–896, 2015.

[13] M. Zhang and S. Kim, "Evaluation of MMSE-Based iterative soft detection schemes for coded massive MIMO system," *IEEE Access*, vol. **7**, pp. 10166–10175, 2019.

[14] J. Yang, C. Zhang, X. Liang, *et al*., "Improved symbol-based belief propagation detection for large-scale MIMO," in *Proc. IEEE Workshop on Signal Processing Systems (SiPS)*, Oct. 2015.

[15] W. Fukuda, T. Abiko, T. Nishimura, *et al*., "Low-complexity detection based on belief propagation in a massive MIMO system," in *Proc. IEEE Vehicular Technology Conf. (VTC)*, June 2013.

[16] T. Takahashi, S. Ibi, S. Sampei, *et al*., "On normalization of matched filter belief in GaBP for large MIMO detection," in *Proc. IEEE Vehicular Technology Conf. (VTC)*, Sept. 2016.

[17] T. Usami, T. Nishimura, T. Ohgane, *et al*., "BP-based detection of spatially multiplexed 16-QAM signals in a fully massive MIMO system," in *Proc. Int. Conf. on Computing, Networking and Communications (ICNC)*, Feb. 2016, pp. 166−170.

[18] P. Som, T. Datta, A. Chockalingam, B. S. Rajan, *et al*., "Improved large-MIMO detection based on damped belief propagation," in *Proc. IEEE Information Theory Workshop on Information Theory*, 2010.

[19] F. Long and T. Lv, "Relaxed belief propagation for MIMO detection," presented at IEEE Int. Symp. on Information Theory (ISIT), July 2011.

[20] J. Yang, W. Song, S. Zhang, *et al*., "Low-Complexity belief propagation detection for correlated large-scale MIMO systems," *J Sign. Process. Syst.*, vol. 90, no, 4, pp. 585–599, 2018.

[21] T. Watabe, T. Nishimura, T. Ohgane, *et al*., "Superposed 16-QAM signal detection using GaBP in a massive MIMO system," in *Proc. APSIPA Annual Summit and Conf.*, Nov. 2018, pp. 1416−1420.

Kazuyuki Sakoda received his Master degree of Science in 2012 from Tokyo Institute of Technology (Tokyo, Japan). He is currently an assistant professor with the Miyakonojo College (Miyazaki, Japan) and pursuing a doctoral degree of Science in Kagoshima University (Kagoshima, Japan). His research interest are wireless communications and nonlinear science. He is a member of The Institute of Electronics, Information and Communication Engineers. He is also a member of The Physical Society of Japan.

Hiroki Hata is associate professor of Graduate School of Science and Engineering, Kagoshima University (Kagoshima, Japan). He received the master's degree and the doctor's degree of Science in Kyushu University (Fukuoka, Japan) in 1987 and 1990. His research interest are nonlinear science and statistical physics. He is a member of The Physical Society of Japan.

Shigefumi Hata obtained a doctoral degree of Science in 2012 from Kyoto University (Kyoto, Japan). He is currently an associate professor in Graduate School of Science and Engineering at Kagoshima University (Kagoshima, Japan). His research interest is nonlinear physics and complex networks. He is a member of The Physical Society of Japan.